HHS Public Access

Author manuscript

Nat Immunol. Author manuscript; available in PMC 2021 July 01.

Published in final edited form as:

Nat Immunol. 2021 January ; 22(1): 25–31. doi:10.1038/s41590-020-00826-9.

Distinct antibody responses to SARS-CoV-2 in children and adults across the COVID-19 clinical spectrum

Stuart P. Weisberg[1,†], **Thomas J. Connors**[2,†], **Yun Zhu**[2,3], **Matthew R. Baldwin**[4], **Wen-hsuan Lin**[1], **Sandeep Wontakal**[1], **Peter A. Szabo**[5], **Steven B. Wells**[6], **Pranay Dogra**[5], **Joshua Gray**[5], **Emma Idzikowski**[2], **Debora Stelitano**[2,3,7], **Francesca T. Bovier**[2,3,7], **Julia Davis-Porada**[8], **Rei Matsumoto**[5,9], **Maya Meimei Li Poon**[5], **Michael Chait**[1,5], **Cyrille Mathieu**[10], **Branka Horvat**[10], **Didier Decimo**[10], **Krystalyn E. Hudson**[1], **Flavia Dei Zotti**[1], **Zachary C. Bitan**[1], **Francesca La Carpia**[1], **Stephen A. Ferrara**[13], **Emily Mace**[2], **Joshua Milner**[2], **Anne Moscona**[2,3,11,12], **Eldad Hod**[1], **Matteo Porotto**[2,3,7,*], **Donna L. Farber**[5,9,11,*]

[1]Department of Pathology and Cell Biology, Columbia University Irving Medical Center, New York, NY 10032

[2]Department of Pediatrics, Columbia University Irving Medical Center, New York, NY 10032

[3]Center for Host-Pathogen Interactions, Columbia University Irving Medical Center, New York, USA

[4]Department of Medicine, Columbia University Irving Medical Center, New York, NY 10032

[5]Columbia Center for Translational Immunology, Columbia University Irving Medical Center, New York, NY 10032

[6]Department of Systems Biology, Columbia University Irving Medical Center, New York, NY 10032

[7]Department of Experimental Medicine, University of Study of Campania ‘Luigi Vanvitelli’, Naples, Italy

Correspondence: Donna L. Farber, df2396@cumc.columbia.edu and Matteo Porotto, mp3509@cumc.columbia.edu.

[†]co-first author

[*]co-senior author

AUTHOR CONTRIBUTIONS

All authors meet authorship criteria and approve of publication. S.P.W., T.J.C., M.P. and D.L.F., A.M., and E.H. conceived and designed the study and assays, wrote and/or edited the paper. T.J.C., M.R.B., D.L.F., E.M., J.M., E.I., coordinated sample acquisition, recruited and consented MIS-C and COVID-ARDS patients. T.J.C., J.D-P., S.P.W., E.M., J.M. and M.R.B. performed compilation and analysis of clinical data from MIS-C and COVID-ARDS patients. E.H., and Z.C.B. recruited and consented convalescent plasma donors. S.P.W. and Z.C.B. performed compilation and analysis of data from the convalescent plasma study. F.L.C., S.A.F, M.C., and S.P.W. performed collection, isolation and storage of samples from convalescent plasma donors. P.A.S, S.B.W., P.D., J.G., E.I., R.M., and M.M.L.P. performed collection, isolation and storage of samples from COVID-ARDS patients. E.H., S.W. K.E.H, F.D.Z. and W.L. established and performed ELISA assays for quantification of anti-SARS-CoV-2 S and N protein IgG, IgM, and IgA from human serum and plasma. M.P., A.M., F.T.B, D.S. and Y.Z. established and performed SARS-CoV-2 S protein pseudovirus neutralization assays. C.M., B.H., and D.D. established and performed the SARS-CoV-2 live virus neutralization assay. S.P.W., D.L.F and T.J.C. performed compilation and analysis of data from the ELISA, pseudovirus neutralization and live virus neutralization assays.

Competing Interests statement

The authors have no conflicts with regard to this work.

Data availability statement

The raw data analyzed for this study are provided as Source Data. Additional supporting data are available from the authors upon request.

Code availability statement

N/A

[8]Medical Scientist Training Program, Columbia University, New York, NY 10032

[9]Department of Surgery, Columbia University Irving Medical Center, New York, NY 10032

[10]CIRI, International Center for Infectiology Research, Inserm, U1111, University Claude Bernard Lyon 1, CNRS, UMR5308, Ecole Normale Supérieure de Lyon, France

[11]Department of Microbiology and Immunology, Columbia University Irving Medical Center, New York, NY 10032

[12]Department of Physiology &Cellular Biophysics, Columbia University Irving Medical Center, New York, NY 10032

[13]School of Nursing, Columbia University Irving Medical Center, New York, NY 10032

INTRODUCTION

Clinical manifestations of COVID-19 caused by the novel coronavirus SARS-CoV-2 are associated with age[1,2]. Adults develop respiratory symptoms, which can progress to Acute Respiratory Distress Syndrome (ARDS) in it most severe form, while children are largely spared from respiratory illness but can develop a life-threatening multisystem inflammatory syndrome (MIS-C)[3–5]. Here, we show distinct antibody responses in children and adults following SARS-CoV-2 infection. Adult COVID-19 cohorts had anti-Spike (S) IgG, IgM and IgA antibodies, as well as anti-Nucleocapsid (N) IgG antibody, while children with and without MIS-C had reduced breadth of anti-SARS-CoV-2-specific antibodies, predominantly generating IgG antibodies specific for the S protein but not for the N protein. Moreover, children with and without MIS-C had reduced neutralizing activity compared to both adult COVID-19 cohorts, indicating a reduced protective serological response. These results suggest a distinct infection course and immune response in children independent of whether they develop MIS-C, with implications for developing age-targeted strategies for testing and protecting the population.

The clinical manifestations of SARS-CoV-2 infection in children are distinct from adults. Children with COVID-19 rarely exhibit severe respiratory symptoms and often remain asymptomatic[2], whereas adults experience respiratory symptoms of varying severity, and older adults and those with comorbidities such as hypertension and diabetes have significantly higher risks of developing COVD-19-associated ARDS with high mortality[2,6]. In children, a rare but severe clinical manifestation of SARS-CoV-2 infection designated Multisystem Inflammatory Syndrome in Children (MIS-C), exhibits similarities to Kawasaki disease in certain inflammatory features and cardiovascular involvement while generally lacking severe respiratory symptoms[3–5]. The nature of the immune response to SARS-CoV-2 in children with different clinical manifestations ranging from asymptomatic to MIS-C relative to the more common respiratory manifestations of COVID-19 in adults, remains unclear.

The generation of virus-specific antibodies which neutralize or block infectivity is the most consistent correlate of protective immunity for multiple infections and vaccines[7,8]. Antibodies specific for the major SARS-CoV-2 antigens, including the Spike (S) protein

which binds the cellular receptor for viral entry, and the nucleocapsid (N) protein necessary for viral replication have been detected in actively infected patients and in patients with mild disease who recovered[9–12]. Anti-S antibodies, in particular, can exhibit potent neutralizing activity and are currently being pursued as a therapeutic option for infusion into patients during severe disease and for targeted generation in vaccines[13–15]. Defining the nature of the antibody response to SARS-CoV-2 infection as a function of age and clinical syndrome can provide essential insights for improved screening and targeted protection for the global population that continues to suffer from this relentless pandemic.

In this study, we investigated the specificity and functionality of the antibody response and its protective capacity in adult and pediatric patients seen at Columbia University Irving Medical Center/NewYork-Presbyterian (CUIMC/NYP) hospital and the Morgan Stanley Children's Hospital of New York (MSCHONY) during the height of the pandemic in New York City from March-June, 2020[3,13,16,17]. We present 4 patient cohorts comprising a total of 79 individuals, including adults recruited as convalescent plasma donors who recovered from mild COVID-19 respiratory disease without requiring hospitalization (CPD, n=19), adults hospitalized with severe COVID-19 Acute Respiratory Distress Syndrome (COVID-ARDS, n=13), and two pediatric cohorts including children hospitalized with MIS-C (MIS-C, n=16) and children who were infected with SARS-CoV-2 but did not develop MIS-C (Pediatric Non-MIS-C, n=31) (See Table 1 for clinical characteristics). The adult cohorts represented a broad age range (19-84 y) while the pediatric subjects were younger (3-18 y) (Table 1). Subjects were diagnosed as infected with SARS-CoV-2 based on history of symptoms, PCR-positive test for virus and/or by serology (Table 1). While co-morbidities were rare among pediatric subjects, they were frequently present in adult subjects with COVID-ARDS (Supplementary Table 1). Samples from COVID-ARDS and MIS-C patients were obtained within 24-36 h of being admitted or intubated for respiratory failure, largely prior to the initiation of therapeutic interventions (Supplementary Table 1). Samples from pediatric Non-MIS-C subjects were obtained during phlebotomy for various clinical reasons, including routine screening for hospital admission and medical procedures (Supplementary Table 2), with 48% having experienced no COVID-like symptoms and designated as asymptomatic. Both MIS-C and COVID-ARDS subjects exhibited markers of systemic inflammation including highly elevated concentrations of interleukin 6 (IL-6) and C-reactive protein (CRP), while ferritin and lactate dehydrogenase (LDH), were significantly increased in COVID-ARDS compared to MIS-C subjects (Table 1). Only 2 pediatric subjects developed respiratory failure and ARDS (Table 1; 1 with MIS-C and 1 non-MIS-C), indicating distinct inflammatory responses and clinical manifestations between children and adults in response to infection.

We quantitated SARS-CoV-2 specific antibodies for each cohort in terms of specificity and antibody class, including IgM generated initially in a primary response and IgG and IgA classes prominent in serum and secretions, respectively. Anti-S antibodies were present as IgG (Fig. 1a), IgM (Fig. 1b) and IgA (Fig. 1c) classes in adult COVID-ARDS and CPD donors, with significantly higher concentration in COVID-ARDS patients for all classes (Fig. 1a–c). By contrast, anti-S antibody titers and isotype predominance in both pediatric cohorts (MIS-C and non-MIS-C) were similar to each other and to the adult CPD subjects—showing predominant anti-S IgG (Fig. 1a), low titers of anti-S IgM (Fig. 1b) (similar to

negative control pre-pandemic plasma), and variable titers of anti-S IgA antibodies (Fig. 1c). We further assessed the specificity of anti-S IgG for SARS-CoV-2 S protein compared to other coronavirus strains using a cell-based ELISA (see methods). Plasma IgG from subject samples but not pre-pandemic control samples bound SARS-CoV-2 S protein and the common circulating D614G S protein variant[18], but did not significantly bind S protein from SARS-CoV-1 or MERS coronaviruses (Extended Data Fig. 1), establishing the specificity of the anti-S IgG response for SARS-CoV-2 in all cohorts. However, the abundance of IgG antibodies specific for the SARS-CoV-2 nucleocapsid (N) protein, which complexes with viral RNA and is involved in viral replication[19] was significantly lower in both pediatric cohorts compared to the two adult cohorts (Fig. 1d). The low amounts of anti-N IgG were similar in children with and without MIS-C, and the higher anti-N IgG titers in adults were similar in the CPD and COVID-ARDS cohort, suggesting that generation of anti-N antibody is age- but not symptom-dependent.

Potential effects of age and time post-symptom onset (i.e., disease course) on the differential antibody abundance for each cohort were examined. While there was no significant correlation between anti-S IgG and age among the adult subjects and the pediatric MIS-C cohort, a modest but significant negative correlation between age and anti-S IgG titers was observed in the pediatric non-MIS-C cohort (Fig. 1e, right). Moreover, there was a significant correlation of anti-N IgG titers with subject age within the CPD group with younger adults having lower anti-N titers than older adults, while both pediatric groups had low anti-N titers across all ages (Fig. 1f). Analysis of antibody abundance as a function of time post-symptom onset revealed a significant correlation between anti-S IgG titers and increased time post-symptom for both pediatric groups and the adult COVID-ARDS group, suggestive of an evolving response over time (Fig. 2a). No correlation with symptom onset and anti-S IgM was observed (Fig. 2b). These results show that the anti-SARS-CoV-2 antibody response generated in children is predominantly anti-S IgG antibodies independent of clinical syndrome. By contrast, adults generate broader antibody responses to infection in terms of isotypes and specificities, and exhibit increased magnitude and breadth of the anti-S antibody response with more severe disease.

The functional capacity of antibodies to provide protection correlates to their neutralizing activity in blocking virus infection. We developed a cell-based pseudovirus assay based on a system previously reported[20,21] in which multi-cycle infection of red fluorescent protein (RFP)-expressing vesicular stomatitis virus (VSV) pseudotyped with SARS-CoV-2 S protein is measured in the presence of serially diluted plasma samples (see Methods). We validated this assay by comparing neutralizing activity of plasma samples tested in the pseudovirus assay to activity measured in live virus microneutralization assay based on inhibition of cytopathic effect[22], and found a direct correlation in neutralizing activity calculated from the pseudovirus and live virus assay over a wide range of neutralizing activity (Fig. 3a).

Neutralizing activity as measured by the pseudovirus assay showed differences between the four cohorts that were associated with age group and/or clinical severity. The pediatric MIS-C and Non-MIS-C groups both exhibited significantly lower neutralizing activity than the adult CPD and COVID-ARDS groups, while plasma from COVID-ARDS patients show the highest neutralizing potency of the four groups across the dilution series (Fig. 3b,c). No

differences were observed in neutralizing activity in the MIS-C compared to the pediatric Non-MIS-C group (Fig. 3b,c). Only a small fraction of antibodies raised against viral antigens will have neutralizing activity against the virus, which correlates with protective capacity[23]. By linear regression, there was significant correlation between the abundance of anti-S IgG and neutralizing activity within the CPD, MIS-C and pediatric Non-MIS-C groups, albeit with a significantly lower elevation and *y*-intercept for MIS-C group relative to the COVID-ARDS and CPD groups (Fig. 3d). Together, these results establish a significant quantitative difference in neutralizing activity of anti-SARS-CoV-2 antibodies between pediatric and adult groups.

We examined potential effects of age and disease course on neutralizing activity in the different groups. There was no correlation between neutralizing activity and patient age in either adult group (Fig. 3d). However, there was a significant decline of neutralizing activity with patient age in the pediatric Non-MIS-C group (Fig. 3e, right) similar to the decrease in anti-S IgG abundance with age observed during the teenage years (Fig. 1e, right). Neutralizing activity within each group did not correlate with time post-symptom onset except in the severely ill COVD-ARDS group (Fig. 4a). Moreover, MIS-C patients also maintained the same titers of anti-S IgG and neutralizing activity 2-4 weeks after hospital discharge based on paired analysis of the follow-up compared to the retested primary sample in 10/16 (62.5%) of the patients (Fig. 4b). Together, these results indicate that lower magnitude of functional antibody responses in pediatric SARS-CoV-2 infection compared to adults is age associated and not related to infection course.

To better define how SARS-CoV-2 antibody responses are related to age and clinical syndrome, we performed multivariable linear regression analysis to control for effects of demographic and clinical covariates. Consistent with the grouped analysis (Fig. 1a–d, 3b), analysis of all pediatric and adult data showed that the pediatric age group is a significant predictor of lower SARS-CoV-2 neutralizing activity, anti-S IgM and anti-N IgG, and these relationships are independent of time post-symptom onset, clinical syndrome or sex (Supplementary Table 3). In addition, ARDS was found to be a significant independent predictor of higher SARS-CoV-2 neutralizing activity, anti-S IgG and anti-S IgM (Supplementary Table 3). Within the subgroup of pediatric subjects, age was found to be a significant independent predictor of SARS-CoV-2 neutralizing activity (Supplementary Table 3), consistent with the pairwise analysis (Fig. 3e, right). These results show that the observed relationships of age and clinical syndrome with SARS-CoV-2 antibody responses are independent of potentially confounding factors, including being male.

Together, our results show quantitative and qualitative differences in the anti-SARS-CoV-2-specific antibody response across the spectrum of infection in children compared to adults. Children exhibited a SARS-CoV-2-specific antibody response that was largely limited to IgG anti-S antibodies with the lowest overall level of neutralizing activity compared to adult COVID-19 cohorts. In addition, children with different disease severities (*i.e.* with or without MIS-C) exhibited similar antibody profiles, while in the adult cohorts, those with the most severe disease (ARDS) had higher abundance, breadth and neutralizing activity of anti-SARS-CoV-2 antibodies compared to adults who recovered from mild disease. While there was an association with increased amounts of anti-S IgG and time post-symptom

onset, age remained the major factor distinguishing antibody profiles. Additionally, the durable responses seen in follow-up samples from MIS-C subjects provide evidence for relative stability of antibody abundance over a period of weeks. These findings suggest distinct primary SARS-CoV-2 infection courses and immune responses in children and adults.

Optimal protection to viral respiratory tract infections is mediated by virus-specific immunological memory developed during previous exposures[24]. The majority of primary exposures, especially to viral respiratory pathogens which are ubiquitous in the population, occur during infancy and childhood and virus-specific memory is established by adult life[25,26]. Consequently, it is largely unknown how primary immune responses to viral pathogens may differ between children and adults. The sudden and widespread emergence of SARS-CoV-2 as a novel pathogen enables the study of primary immune responses across all ages. The reduced respiratory symptoms and low incidence of ARDS in the pediatric population[2] suggest a distinct infection course, possibly due to lower expression of the viral receptor (ACE2) in pediatric airway epithelial cells[27] or a more robust innate immune response in children[28–30]. A milder infection course in pediatric groups is further consistent with lower abundance of anti-N-specific antibodies identified here, as release of N proteins requires lysis of virally infected cells. The age association of anti-N antibodies in the adult CPD group is consistent with the age-associated risk for more severe and prolonged disease from SARS-CoV-2 infection. While current platforms to determine prior infection with SARS-CoV-2 rely heavily on the detection of anti-N IgG, our results suggest that these testing platforms may have decreased sensitivity for assessing previous infections among the pediatric population.

The reduced functional antibody response in children compared to adults could also be due to efficacious immune-mediated viral clearance resulting in fewer respiratory symptoms and severe illness. The presence of SARS-CoV-2-specific T cells in the peripheral blood of recovered and COVID-ARDS adults has been demonstrated in multiple cohorts[31–33], though the protective capacity of these T cells is unclear. The pediatric T cell response to SARS-CoV-2 requires investigation but may exceed the adult responses due to an increased number of naïve T cells available to respond to new pathogens[34], or more recently acquired T cell memory to related coronavirus strains[35] due to children experiencing more respiratory illnesses. The IgG predominance in the majority of children examined here is consistent with pre-existing immunological memory. Interestingly, less severe manifestations of COVID-19 have been associated with a more coordinated adaptive immune responses in adults[36], suggesting that the quality and quantity of the immune response is important for protection from severe disease, which are important future areas of investigation for understanding the immune response to SARS-CoV-2 infection in children.

The similar antibody profiles in children with and without MIS-C suggests that the adaptive immune response per se, is not associated with MIS-C pathogenesis. However, reduced neutralizing activity may predispose children to develop low-level, persistent infection in other sites resulting in MIS-C. Children can present with gastrointestinal symptoms rather than respiratory illness and demonstrate prolonged fecal shedding of the virus[37]. Alternately, the presence of non-neutralizing anti-S Abs could lead to antibody-dependent enhancement

of infection (ADE) known to occur in viral infections including SARS-CoV-1[38]. Additionally, autoreactive antibodies recently identified in children with MIS-C may promote aberrant immune responses leading to systemic inflammation[29,30]. Further studies delineating the differences in adult and pediatric immune responses to SARS-CoV-2 are warranted to define how protection or pathology is mediated in response to this pathogen. In summary, our results suggest a distinct infection course and immune response in children independent of whether they develop MIS-C, with implications for developing age-targeted strategies for testing and protecting the population.

METHODS

Subjects

We recruited a total of 79 subjects from MSCHONY and CUIMC/NYP who represented distinct clinical manifestations of SARS-CoV-2 infection and different age groups divided into four cohorts: 1. Individuals (n=19) donating blood as part of our institution's convalescent plasma trial (convalescent plasma donors, CPD) following a history of recent illness consistent with COVID-19 but not requiring hospitalization and subsequently identified as positive for anti-SARS-CoV-2 antibodies; 2. Patients with severe COVID-19 and ARDS (n=13) who tested positive for SARS-CoV-2 by polymerase chain reaction (PCR) from nasopharyngeal swabs; 3. Pediatric patients with MIS-C (n=16) and confirmed SARS-CoV-2 antibody positive serology; and 4. Pediatric patients without MIS-C (n=31) receiving medical attention at CUIMC/NYP and confirmed to have active or previous SARS-CoV-2 infection by PCR from nasopharyngeal swabs or antibody positive serology. ARDS was defined by clinical consensus criteria; including infiltrates on chest radiograph and a PaO2/FiO2 ratio of less than 300, or pediatric criteria equivalent [39,40]. MIS-C was defined using the Center for Disease Control definition; <21 years of age, fever >38°C for >24 h, laboratory evidence of inflammation, hospital admission, multisystem involvement, no alternative plausible diagnosis, and positive SARS-Cov-2 serology[41]. Sequential Organ Failure Assessment (SOFA) scores were calculated on all hospitalized subjects using previously validated adult and pediatric score tools to provide additional clinical insight into subject disease severity[42–44]. This study was approved by the Institutional Review Board at CUIMC. Written consent was obtained from CPD subjects. Due to the limitations placed on direct contact with infected subjects and a need to conserve personal protective equipment, verbal informed consent was obtained from surrogates of critically ill COVID-ARDS subjects and verbal parental consent was obtained for MIS-C subjects. Biospecimens and data from Non-MIS-C pediatric patients were obtained from the Columbia University Biobank (CUB).

Sample Processing

Blood samples were obtained at time of outpatient donation for CPD subjects, at time of admission for MIS-C subjects, during clinical care for pediatric Non-MIS-C subjects and following diagnosis of ARDS for COVID-ARDS patients. Plasma was isolated from whole blood via centrifugation. Aliquots were frozen at −80°C prior to analysis.

Purification of SARS-CoV-2 viral proteins

The ectodomain of the SARS-CoV-2 spike trimer[45] was cloned into mammalian expression vector pCAGGS (Addgene), with a fold-on tag followed by 6×His tag and Strep tag II at the C-terminal. This expression vector was transiently transfected into HEK293F cells and the spike trimer secreted in the supernatant was purified 3-5 days post transfection by metal-affinity chromatography using an Ni-NTA (Qiagen) column. SARS-CoV-2 nucleocapsid protein (N) was cloned into pET28a(+) vector (Millipore-Sigma) with an AAALE linker and 6×His tag at the C-terminal. The NP construct was then used to transform into *Escherichia coli* BL21 (DE3) pLysS cells and the target protein was produced and purified from the bacterial lysate by metal affinity chromatography using an Ni-NTA (Qiagen) column, followed by size-exclusion chromatography on a Superdex 200 10/300 GL column.

Enzyme-linked immunosorbent assay (ELISA) for detection of virus-specific antibodies

SARS-CoV-2 spike trimer and N were coated on 96-well ELISA plates at 4 °C overnight, and unbound proteins were then removed washing with PBS, following by blocking with PBS/3% non-fat dry milk. Plasma samples were serially diluted in PBST (0.1% Tween-20 in PBS) + 10% bovine calf serum starting with 1:100, and five successive four-fold dilutions into each well of the coated plate which was incubated at 37 °C for 1 h, followed by washing 6 times with PBST. Peroxidase affiniPure goat anti-human IgG (H+L) antibody (1:3,000 dilution), anti-human IgM antibody (1:10,000 dilution) (Jackson Immune Research), or anti-human IgA antibody (1:5,000 dilution) (Thermofisher) was subsequently added into each well and incubated for 1 h at 37 °C, washed and Tetramethylbenzidine substrate (Sigma) was added and the reaction was stopped using 1 M sulfuric acid. Absorbance was measured at 450 nm and expressed as an optical density, or OD_{450} value. Identical serial dilutions were performed for all samples with no missing titrations.

Pseudovirus neutralization assay

We adapted a pseudovirus-based neutralization strategy we previously developed to measure inhibition of infection by high biocontainment enveloped viruses in a large number of samples under low-level biocontainment[20,21]. For this assay, SARS-CoV-2 S protein is pseudotyped onto recombinant vesicular stomatitis virus (VSV) that expresses red fluorescent protein (RFP) but does not express the VSV attachment protein, G (VSV-ΔG-RFP). Initially, VSV-ΔG-RFP pseudotyped with VSV G is used to infect 293T (human kidney epithelial) cells that were co-transfected with full-length codon optimized SARS-CoV-2 S-protein (Epoch Life Science), the viral entry receptor ACE2 (Epoch Life Science) and green-fluorescent protein (GFP). Infected HEK293T cells are then mixed at a 2 to 1 ratio with Vero (African green monkey kidney) cells, which have high endogenous expression of ACE2[46]. The cells are then combined with diluted serum or plasma in 96-well plates. During the assay, infected S protein-expressing HEK293T cells generate VSV-ΔG-RFP viruses that bear S protein which subsequently infects and drives RFP expression in Vero cells and undergo multiple cycles of entry and budding in the HEK293T cells due to the co-expression of S protein with ACE2. The GFP and RFP signals are measured 24–48 h after plating (Infinite M1000 PRO microplate reader, Tecan), resulting in robust amplification of the S protein pseudovirus-driven RFP signal between 24–48 h. Inhibition of

RFP signal amplification indicates S protein neutralizing activity in patient plasma (Extended Data Fig. 1). Identical, five-fold serial dilutions were performed for all samples and there were no missing titration data points for any of the samples.

SARS-CoV-2 viral stock production

SARS-CoV-2 (2019-nCoV/USA_WA1/2020) was kindly provided to B.H. by World Reference Center for Emerging Viruses and Arboviruses (WRCEVA). To generate virus stocks, Vero E6 cells (kindly provided by F. Cosset, CIRI - International Center for Infectiology Research, Inserm) were inoculated with virus at a MOI of 0.01. The virus-containing medium was harvested at 72 h post infection, clarified by low-speed centrifugation, aliquoted, and stored at −80°C. Virus stock was quantified by limiting dilution plaque assay on Vero E6 cells as described[47,48].

Live virus neutralization assay

Two-fold dilutions of plasma in 50 μL of Dulbecco's Modified Eagle Media (DMEM) were incubated with 200 plaque forming units (PFU) of SARS-CoV-2 in 50 μL of DMEM for 30 min at 4 °C. 100 μL of DMEM 4%FBS containing 4×10^4 Vero E6 cells were added on the top of the former mix in order to have final dilution of sera from 1:50 to 1:6400 (4 wells per dilution). Cells were then incubated for 3 days at 37 °C, 5% CO_2. Cytopathic effect was revealed by crystal violet staining, and scored by an observer blinded to the study design and sample identity. Neutralization end point titers were expressed as the value of the last serum dilution that completely inhibited virus-induced cytopathic effect.

Quantitation of antibody titrations in ELISA and neutralization assays

For quantitation of neutralization titers in the pseudovirus assay, RFP signal driven by the pseudovirus normalized to the GFP signal derived from the SARS-Cov-2 S protein and ACE2 transfected cells was measured at 24 and 48 h; the ratio of normalized RFP at 48 h (RFP48) to normalized RFP at 24 h (RFP24) was calculated. This ratio provides a read-out of multicycle infection of the S protein/ACE2 transfected cell monolayer by S protein-bearing pseudoviruses. Neutralizing activity for each sample was calculated by taking the sum of the reciprocal of the RFP48/RFP24 ratio at all 6 plasma dilutions for each sample as described[49], and also by percent inhibition of multicycle replication at each dilution calculated based on the RFP48/RFP24 ratio of the sample, control wells of maximal multicycle replication without inhibition (MAX) and control wells with 100% inhibition of multicycle replication using a lipidated SARS-CoV-2 derived peptide (MIN)[50,51]. The equation for % inhibition of multicycle replication: 100 × (1-(sample- MAX)/(MAX – MIN)).

Statistical analysis

All statistical analysis was performed using Prism software version 8.4.3 (GraphPad). Comparisons of clinical data between groups was performed using the Mann–Whitney U test and one-way Analysis of Variance (ANOVA) and Dunn's multiple comparisons test. Comparisons of antibody levels and neutralization activity were performed using one-way ANOVA and Tukey's multiple comparisons test. Pairwise correlation analysis was

performed using simple linear regression. Multiple linear regression analysis was performed on the combined adult and pediatric data as well as the adult and pediatric cohorts individually. For all analyses, outcome variables included the abundance of anti-S IgG, anti-S IgM, anti-N IgG and SARS-CoV-2 neutralizing activity. For the combined adult and pediatric dataset, the independent variable is pediatric age group ('Pediatric') and covariates include sex, clinical syndrome and time post symptom onset (days). For the adult and pediatric subgroup analyses, the independent variables are clinical syndrome and age (years), and covariates include sex and time post symptom onset (days). For each variable, P values were calculated using the *t* statistic with two-sided hypothesis testing.

Extended Data

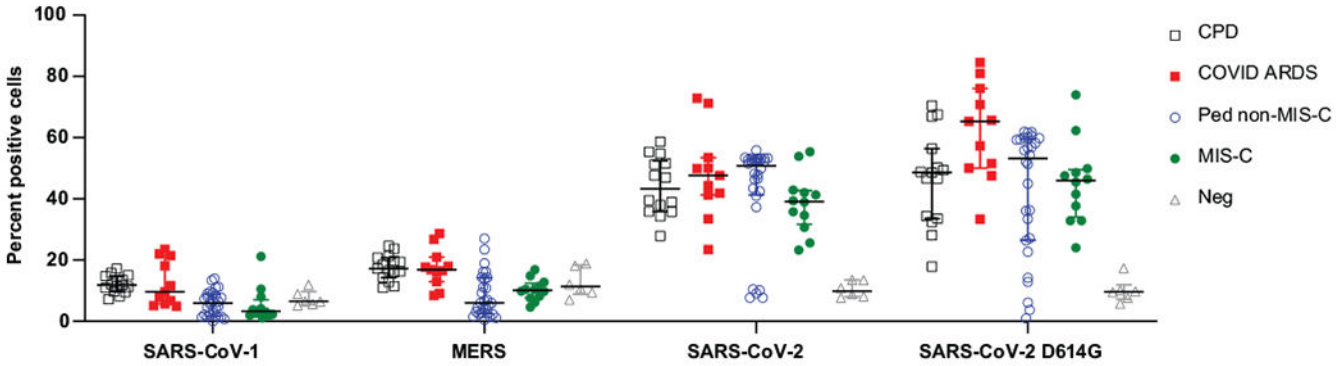

Extended Data Fig. 1. Specificity of subjects' antibodies for SARS-CoV-2 S protein.

The specificity of antibodies for SARS-CoV-2 S protein compared to SARS-CoV-1 and MERS S protein was assayed in a cell-based IgG binding assay. HEK293T cells were transfected with S protein and its common variants from the indicated coronaviruses. The transfected cells were then incubated with human plasma from the indicated study groups and bound human IgG was detected using fluorescently tagged protein G (Methods). Shown are the percentage of the S protein transfected cells that are positive for human IgG in each patient group: CPD, black squares, n = 19; COVID-ARDS, red squares, n = 13; pediatric non-MIS-C, n = 28; MIS-C, green circles, n = 16; and control plasma from pre-pandemic donors (grey triangles; Neg, n = 6). Black bar indicates the median+interquartile range. P values were calculated by one-way ANOVA with Dunnett's multiple comparisons test (CPD, SARS-CoV-2 vs. SARS-CoV-1: P = 0, SARS-CoV-2 vs. MERS: P = 0; COVID-ARDS, SARS-CoV-2 vs. SARS-CoV-1: P = 0, SARS-CoV-2 vs. MERS: P = 0; Ped non-MIS-C, SARS-CoV-2 vs. SARS-CoV-1: P = 0, SARS-CoV-2 vs. MERS: P = 0; MIS-C, SARS-CoV-2 vs. SARS-CoV-1: P = 0, SARS-CoV-2 vs. MERS: P = 0; Negative control, SARS-CoV-2 vs. SARS-CoV-1: P = 0.32, SARS-CoV-2 vs. MERS: P = 0.52).

Supplementary Material

Refer to Web version on PubMed Central for supplementary material.

ACKNOWLEDGEMENTS

We thank F. Cosset for the donation of Vero E6 cells. We wish to express our gratitude to the Medical ICU nurse champions, C. Garcellano, T. Drukdak, H. Avila Raymundo, L. Wagner, and R. Lee, who led the efforts to obtain patient samples for the adult ARDS patients, to E. Hernandez and L. Gomez for their roles as clinical coordinators, and to the nurses and clinical staff in the Pediatric Intensive Care Unit of MSCHONY. We acknowledge the dedication, commitment, and sacrifice of the other nurses, providers, and personnel who helped care for these patients during the COVID-19 crisis. We acknowledge the suffering and loss of our COVID-19 patients and of their families and our community.

Funding/Support

This work was supported by NIH grants AI128949, AI100119, AI106697 awarded to D.L.F., NIH grants AI121349, NS091263, NS105699, and AI146980 awarded to M.P., and AI114736 awarded to A.M. S.W. is supported by NIH K08DK122130; T.J.C. is supported by NIH K23 AI141686.

Role of the Funder:

The funders/sponsors had no role in the design and conduct of the study; collection, management, analysis, and interpretation of the data; preparation, review, or approval of the manuscript; and decision to submit the manuscript for publication.

REFERENCES

1. Dong Y, et al. Epidemiology of COVID-19 Among Children in China. Pediatrics 145(2020).
2. Wu Z & McGoogan JM Characteristics of and Important Lessons From the Coronavirus Disease 2019 (COVID-19) Outbreak in China: Summary of a Report of 72314 Cases From the Chinese Center for Disease Control and Prevention. JAMA 323, 1239–1242 (2020). [PubMed: 32091533]
3. Cheung EW, et al. Multisystem Inflammatory Syndrome Related to COVID-19 in Previously Healthy Children and Adolescents in New York City. JAMA 324, 294–296 (2020). [PubMed: 32511676]
4. Feldstein LR, et al. Multisystem Inflammatory Syndrome in U.S. Children and Adolescents. N Engl J Med 383, 334–346 (2020). [PubMed: 32598831]
5. Whittaker E, et al. Clinical Characteristics of 58 Children With a Pediatric Inflammatory Multisystem Syndrome Temporally Associated With SARS-CoV-2. JAMA 324, 259–269 (2020). [PubMed: 32511692]
6. Singh AK, et al. Prevalence of co-morbidities and their association with mortality in patients with COVID-19: A systematic review and meta-analysis. Diabetes Obes Metab (2020).doi: 10.1111/dom.14124
7. Lanzavecchia A, Fruhwirth A, Perez L & Corti D Antibody-guided vaccine design: identification of protective epitopes. Curr Opin Immunol 41, 62–67 (2016). [PubMed: 27343848]
8. Corti D & Lanzavecchia A Broadly neutralizing antiviral antibodies. Annu Rev Immunol 31, 705–742 (2013). [PubMed: 23330954]
9. Wang X, et al. Neutralizing Antibodies Responses to SARS-CoV-2 in COVID-19 Inpatients and Convalescent Patients. Clin Infect Dis (2020).doi: 10.1093/cid/ciaa721
10. Ni L, et al. Detection of SARS-CoV-2-Specific Humoral and Cellular Immunity in COVID-19 Convalescent Individuals. Immunity 52, 971–977 e973 (2020). [PubMed: 32413330]
11. Long QX, et al. Antibody responses to SARS-CoV-2 in patients with COVID-19. Nat Med 26, 845–848 (2020). [PubMed: 32350462]
12. Amanat F, et al. A serological assay to detect SARS-CoV-2 seroconversion in humans. Nat Med 26, 1033–1036 (2020). [PubMed: 32398876]

13. Bloch EM, et al. Deployment of convalescent plasma for the prevention and treatment of COVID-19. J Clin Invest 130, 2757–2765 (2020). [PubMed: 32254064]
14. Amanat F & Krammer F SARS-CoV-2 Vaccines: Status Report. Immunity 52, 583–589 (2020). [PubMed: 32259480]
15. Huang AT, et al. A systematic review of antibody mediated immunity to coronaviruses: kinetics, correlates of protection, and association with severity. Nat Commun 11, 4704 (2020). [PubMed: 32943637]
16. Cummings MJ, et al. Epidemiology, clinical course, and outcomes of critically ill adults with COVID-19 in New York City: a prospective cohort study. Lancet 395, 1763–1770 (2020). [PubMed: 32442528]
17. Zachariah P, et al. Epidemiology, Clinical Features, and Disease Severity in Patients With Coronavirus Disease 2019 (COVID-19) in a Children's Hospital in New York City, New York. JAMA Pediatr, e202430 (2020). [PubMed: 32492092]
18. Korber B, et al. Tracking Changes in SARS-CoV-2 Spike: Evidence that D614G Increases Infectivity of the COVID-19 Virus. Cell 182, 812–827 e819 (2020). [PubMed: 32697968]
19. Cong Y, et al. Nucleocapsid Protein Recruitment to Replication-Transcription Complexes Plays a Crucial Role in Coronaviral Life Cycle. J Virol 94, e01925–19 (2020).doi: 10.1128/JVI.01925-19 [PubMed: 31776274]
20. Talekar A, et al. Rapid screening for entry inhibitors of highly pathogenic viruses under low-level biocontainment. PLoS One 7, e30538 (2012). [PubMed: 22396728]
21. Porotto M, et al. Simulating henipavirus multicycle replication in a screening assay leads to identification of a promising candidate for therapy. J Virol 83, 5148–5155 (2009). [PubMed: 19264786]
22. Chan KH, et al. Cross-reactive antibodies in convalescent SARS patients' sera against the emerging novel human coronavirus EMC (2012) by both immunofluorescent and neutralizing antibody tests. J Infect 67, 130–140 (2013). [PubMed: 23583636]
23. Gao Q, et al. Development of an inactivated vaccine candidate for SARS-CoV-2. Science 369, 77–81 (2020). [PubMed: 32376603]
24. Kohlmeier JE & Woodland DL Immunity to respiratory viruses. Annu Rev Immunol 27, 61–82 (2009). [PubMed: 18954284]
25. He XS, et al. Analysis of the frequencies and of the memory T cell phenotypes of human CD8+ T cells specific for influenza A viruses. J Infect Dis 187, 1075–1084 (2003). [PubMed: 12660922]
26. PrabhuDas M, et al. Challenges in infant immunity: implications for responses to infection and vaccines. Nat Immunol 12, 189–194 (2011). [PubMed: 21321588]
27. Bunyavanich S, Do A & Vicencio A Nasal Gene Expression of Angiotensin-Converting Enzyme 2 in Children and Adults. JAMA 323, 2427–2429 (2020). [PubMed: 32432657]
28. Pierce CA, et al. Immune responses to SARS-CoV-2 infection in hospitalized pediatric and adult patients. Sci Transl Med 12, eabd5487 (2020). [PubMed: 32958614]
29. Gruber CN, et al. Mapping Systemic Inflammation and Antibody Responses in Multisystem Inflammatory Syndrome in Children (MIS-C). Cell (2020).doi: 10.1016/j.cell.2020.09.034
30. Consiglio CR, et al. The Immunology of Multisystem Inflammatory Syndrome in Children with COVID-19. Cell (2020).doi: 10.1016/j.cell.2020.09.016
31. Weiskopf D, et al. Phenotype and kinetics of SARS-CoV-2-specific T cells in COVID-19 patients with acute respiratory distress syndrome. Sci Immunol 5, eabd2071 (2020). [PubMed: 32591408]
32. Grifoni A, et al. Targets of T Cell Responses to SARS-CoV-2 Coronavirus in Humans with COVID-19 Disease and Unexposed Individuals. Cell 181, 1489–1501 e1415 (2020). [PubMed: 32473127]
33. Sekine T, et al. Robust T Cell Immunity in Convalescent Individuals with Asymptomatic or Mild COVID-19. Cell 183, 158–168 e114 (2020). [PubMed: 32979941]
34. Kumar BV, Connors TJ & Farber DL Human T Cell Development, Localization, and Function throughout Life. Immunity 48, 202–213 (2018). [PubMed: 29466753]
35. Mateus J, et al. Selective and cross-reactive SARS-CoV-2 T cell epitopes in unexposed humans. Science 370, 89–94 (2020). [PubMed: 32753554]

36. Moderbacher C, et al. Antigen-Specific Adaptive Immunity to SARS-CoV-2 in Acute COVID-19 and Associations with Age and Disease Severity. Cell (2020).doi:10.1016/j.cell.2020.09.038

37. Xu Y, et al. Characteristics of pediatric SARS-CoV-2 infection and potential evidence for persistent fecal viral shedding. Nat Med 26, 502–505 (2020). [PubMed: 32284613]

38. Iwasaki A & Yang Y The potential danger of suboptimal antibody responses in COVID-19. Nat Rev Immunol 20, 339–341 (2020). [PubMed: 32317716]

Methods-only References

39. Ranieri VM, et al. Acute respiratory distress syndrome: the Berlin Definition. JAMA 307, 2526–2533 (2012). [PubMed: 22797452]

40. Khemani RG, Smith LS, Zimmerman JJ, Erickson S & Pediatric Acute Lung Injury Consensus Conference, G. Pediatric acute respiratory distress syndrome: definition, incidence, and epidemiology: proceedings from the Pediatric Acute Lung Injury Consensus Conference. Pediatr Crit Care Med 16, S23–40 (2015). [PubMed: 26035358]

41. CDC. Multisystem Inflammatory Syndrome in Children (MIS-C) Associated with Coronavirus Disease 2019 (COVID-19). Vol. 2020 Health Alert Network (Health and Human Services, 2020).

42. Singer M, et al. The Third International Consensus Definitions for Sepsis and Septic Shock (Sepsis-3). JAMA 315, 801–810 (2016). [PubMed: 26903338]

43. Matics TJ & Sanchez-Pinto LN Adaptation and Validation of a Pediatric Sequential Organ Failure Assessment Score and Evaluation of the Sepsis-3 Definitions in Critically Ill Children. JAMA Pediatr 171, e172352 (2017). [PubMed: 28783810]

44. Vasilevskis EE, et al. Validity of a Modified Sequential Organ Failure Assessment Score Using the Richmond Agitation-Sedation Scale. Crit Care Med 44, 138–146 (2016). [PubMed: 26457749]

45. Wrapp D, et al. Cryo-EM structure of the 2019-nCoV spike in the prefusion conformation. Science 367, 1260–1263 (2020). [PubMed: 32075877]

46. Hoffmann M, et al. SARS-CoV-2 Cell Entry Depends on ACE2 and TMPRSS2 and Is Blocked by a Clinically Proven Protease Inhibitor. Cell 181, 271-280 e278 (2020). [PubMed: 32142651]

47. Guillaume V, et al. Nipah virus: vaccination and passive protection studies in a hamster model. J Virol 78, 834–840 (2004). [PubMed: 14694115]

48. Mathieu C, et al. Nipah virus uses leukocytes for efficient dissemination within a host. J Virol 85, 7863–7871 (2011). [PubMed: 21593145]

49. Hartman H, Wang Y, Schroeder HW Jr. & Cui X Absorbance summation: A novel approach for analyzing high-throughput ELISA data in the absence of a standard. PLoS One 13, e0198528 (2018). [PubMed: 29883460]

50. Pessi A, et al. A general strategy to endow natural fusion-protein-derived peptides with potent antiviral activity. PLoS One 7, e36833 (2012). [PubMed: 22666328]

51. Xia S, et al. Fusion mechanism of 2019-nCoV and fusion inhibitors targeting HR1 domain in spike protein. Cell Mol Immunol 17, 765–767 (2020). [PubMed: 32047258]

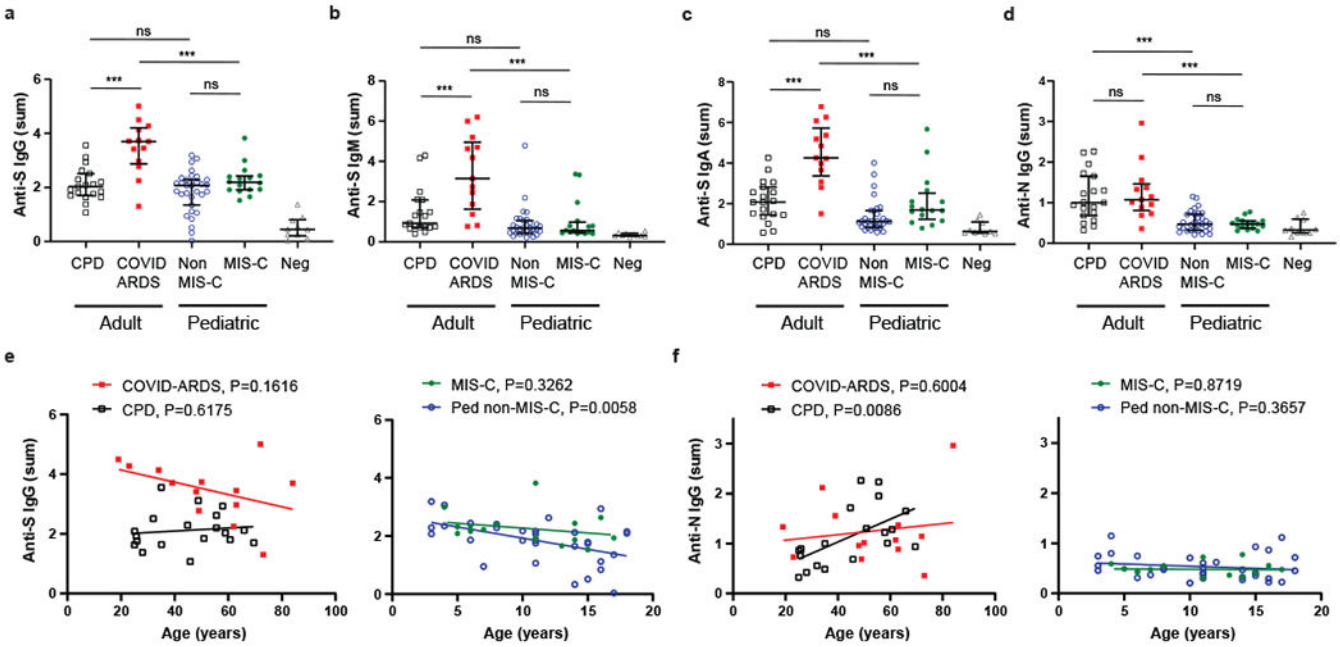

Figure 1. Children with and without MIS-C exhibit distinct SARS-CoV-2 antibody profiles compared to adults with COVID-19.

Levels of antibodies to SARS-CoV-2 spike (S) and nucleocapsid (N) proteins were measured using serial dilutions of patient plasma in an indirect ELISA assay to detect anti-S IgG (a), anti-S IgM (b), anti-S Ig A (c) and anti-N IgG (d). Shown is the absorbance sum across 6 serial 1:4 plasma dilutions from adult convalescent plasma donors (CPD, open black squares, n=19); adult patients with COVID-19 induced acute respiratory distress syndrome (COVID-ARDS, closed red squares, n=13); pediatric patients with a history of SARS-CoV-2 infection but not MIS-C (Non-MIS-C, open blue circles, n=31); patients with MIS-C (MIS-C, closed green circles, n=16); and control plasma from pre-pandemic donors (Neg, grey triangles, n=10). Black bar indicates the median+interquartile range. P values were calculated by one-way ANOVA with Sidak's multiple comparisons test. Anti-S IgG (a), CPD vs. COVID ARDS: $P=1.32\times10^{-4}$, CPD vs. Ped non-MIS-C: P=0.59, COVID ARDS vs. MIS-C: $P=8.53\times10^{-6}$, Ped non-MIS-C vs. MIS-C: P=0.24. Anti-S IgM (b), CPD vs. COVID ARDS: $P=6.93\times10^{-5}$, CPD vs. Ped non-MIS-C: P=0.33, COVID ARDS vs. MIS-C: $P=2.54\times10^{-6}$, Ped non-MIS-C vs. MIS-C: P=0.99. Anti-S IgA (c), CPD vs. COVID ARDS: $P=3.82\times10^{-7}$, CPD vs. Ped non-MIS-C: P=0.08, COVID ARDS vs. MIS-C: $P=9.06\times10^{-7}$, Ped non-MIS-C vs. MIS-C: P=0.11. Anti-N IgG (d), CPD vs. COVID ARDS: P=0.93, CPD vs. Ped non-MIS-C: $P=3.31\times10^{-5}$, COVID ARDS vs. MIS-C: $P=3.88\times10^{-5}$, Ped non-MIS-C vs. MIS-C: P=0.99. Significance is indicated as *P < 0.05, **P < 0.01, ***P < 0.001 or P>0.05 (ns). For anti-S IgG (e) and anti-N IgG (f), subject antibody levels are also plotted against patient age within the adult (left) and pediatric cohorts (right) with the best fit lines and P values calculated using simple linear regression. Anti-S IgG vs. Age (Ped non-MIS-C: R2=0.23, slope=−0.077, y-int=2.70). Anti-N IgG vs. Age (CPD: R2=0.34, slope=0.023, y-int=0.12).

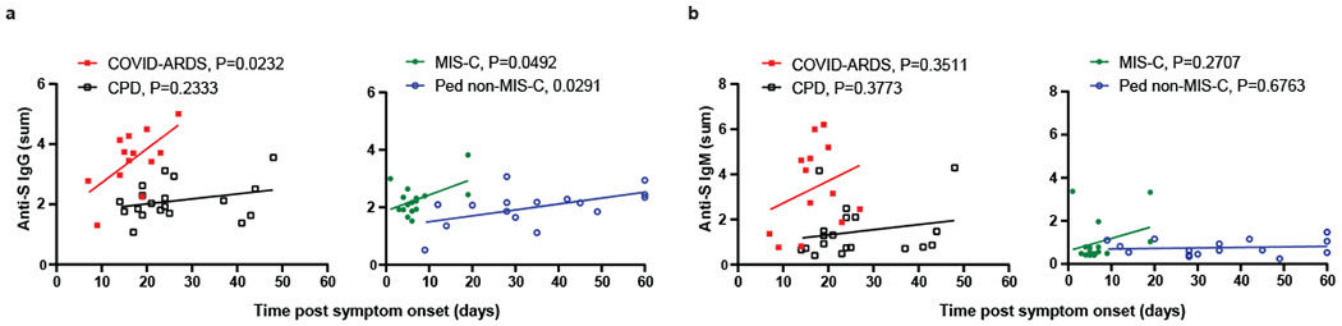

Figure 2. Relationship of anti-S IgG and IgM levels with time post symptom onset for pediatric and adult cohorts.

Levels of anti-S IgG (a), and IgM (b) were plotted against the time post symptom onset for those subjects that were symptomatic either with COVID-19 or MIS-C. The adult groups, CPD (open black squares, n=19) and COVID-ARDS closed red squares, n=13) are plotted on the left and the pediatric groups, MIS-C (closed green circles, n=16) and non-MIS-C (open blue circles, n=16) are plotted on the right with the best fit line and P value, reported to 4 decimal places, was calculated using simple linear regression. Anti-S IgG vs. Time post symptom onset (COVID-ARDS: R2=0.39, slope=0.11, y-int=1.59; MIS-C: R2=0.25, slope=0.055, y-int=1.87; Ped non-MIS-C: R2=0.30, slope=0.021, y-int=1.29).

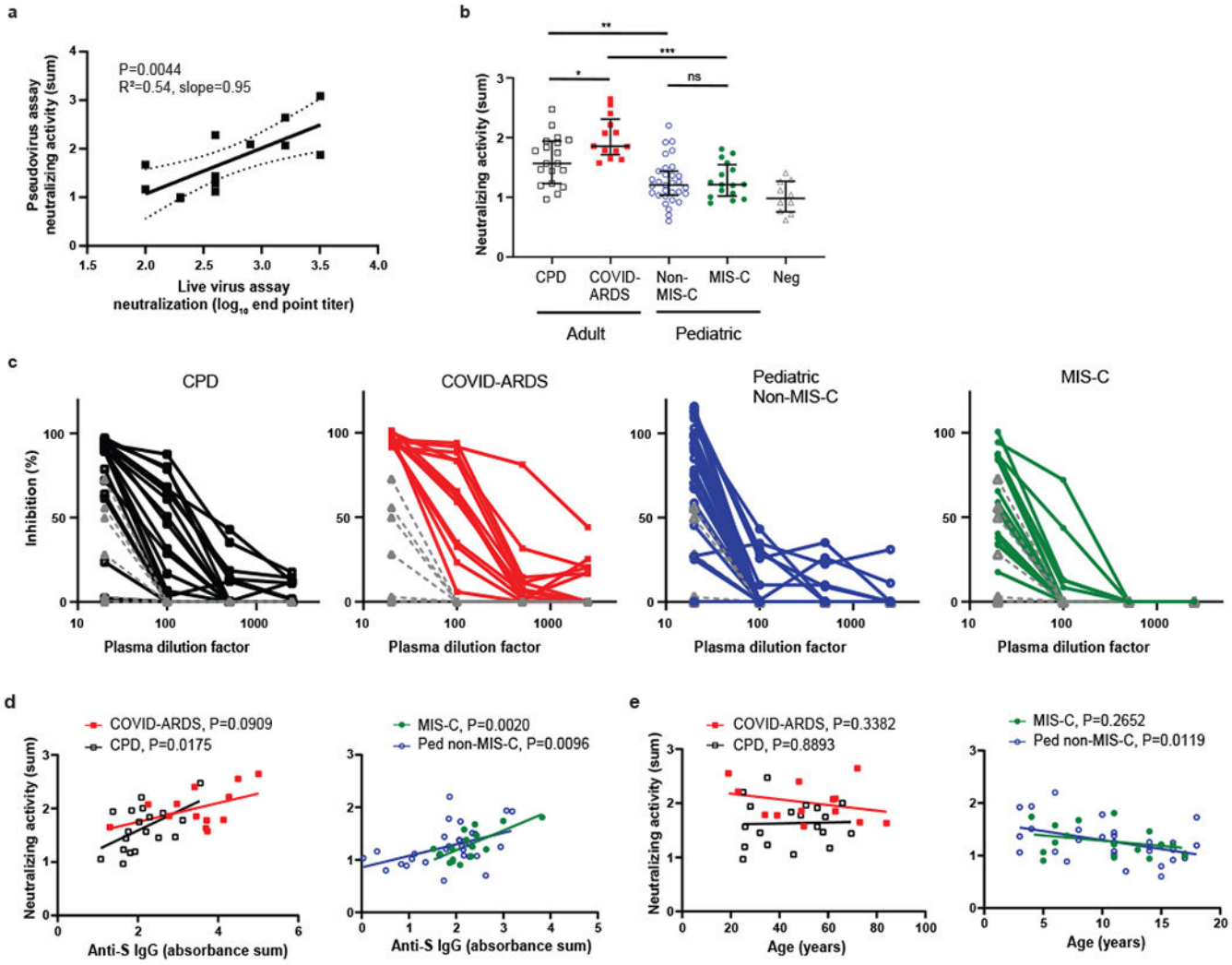

Figure 3. Reduced SARS-CoV-2 neutralizing activity in children with and without MIS-C compared to adults with mild and severe COVID-19.

a, Plasma neutralizing activity in the pseudovirus assay was correlated with the end point titers in a live virus microneutralization assay based on inhibition of cytopathic effect (n=13, see methods), b, Neutralizing activity for SARS-CoV-2-specific antibodies was determined using the pseudovirus assay (see methods). Neutralizing activity is shown from adult convalescent plasma donors (CPD, open black squares, n=19); adult patients with COVID-19 induced acute respiratory distress syndrome (COVID-ARDS, closed red squares, n=13); pediatric patients with a history of SARS-CoV-2 infection but not MIS-C (Non-MIS-C, open blue circles, n=31); patients with MIS-C (MIS-C, closed green circles, n=16); and control plasma from pre-pandemic donors (Neg, grey triangles, n=10). Black bar indicates the median+interquartile range. The P values were calculated by one-way ANOVA with Sidak's multiple comparisons test (CPD vs. COVID ARDS: P=0.019, CPD vs. Ped non-MIS-C: P=0.0031, COVID ARDS vs. MIS-C: $P=3.35x10^{-6}$, Ped non-MIS-C vs. MIS-C: P=1.0). Significance is indicated as *P < 0.05, **P < 0.01, ***P < 0.001 or P>0.05 (ns). Shown (c) are the percent inhibition values of S-protein mediated pseudoviral replication

plotted against the plasma dilution factors for all subjects in each group. Neutralizing activity is plotted against anti-S IgG levels (d) and patient age (e) within the adult (left) and pediatric cohorts (right). The best fit lines and P values (reported to 4 decimal places), were calculated using simple linear regression. Neutralizing activity vs. anti-S IgG (CPD: R2=0.29, slope=0.36, y-int=0.88; MIS-C: R2=0.51, slope=0.38, y-int=0.43; Ped non-MIS-C: R2=0.21, slope=0.22, y-int=0.86). Neutralizing activity vs. age (Ped non-MIS-C: R2=0.20, slope=−0.034, y-int=1.64).

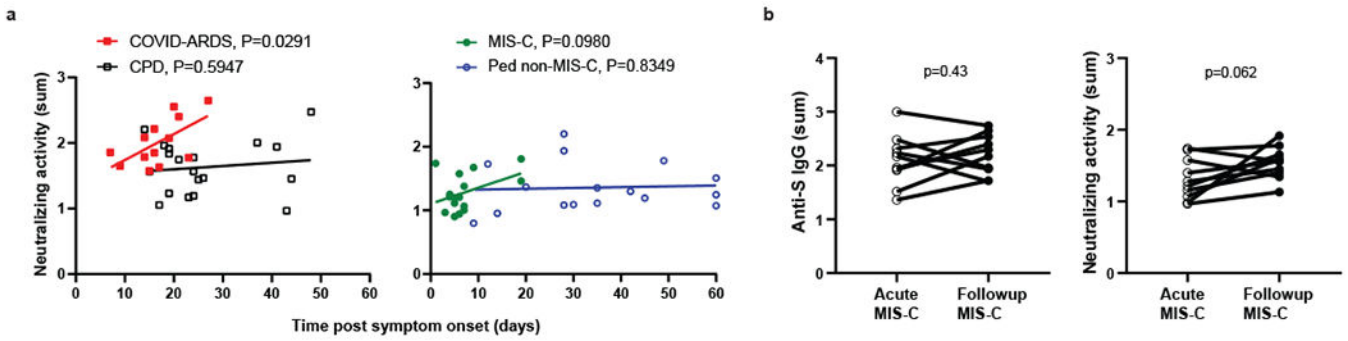

Figure 4. Relationship of anti-SARS-CoV-2 neutralizing activity with time post symptom onset.

a, Levels of neutralization activity were plotted against the time post symptom onset for those subjects that were symptomatic either with COVID-19 or MIS-C. The adult groups, CPD (open black squares, n=19) and COVID-ARDS closed red squares, n=13) are plotted on the left and the pediatric groups, MIS-C (closed green circles, n=16) and non-MIS-C (open blue circles, n=16) are plotted on the right with the best fit line and P value calculated using simple linear regression (COVID-ARDS: R2=0.36, slope=0.040, y-int=1.34). b, The anti-S IgG levels (left) and neutralizing activity (right) of MIS-C subjects (n=10) during the acute phase of illness and at a follow-up visit 2–4 weeks after hospital discharge. The P values were calculated by two way paired t-test.

Table 1.

Demographic and Clinical Data

	Adults		Pediatric		
	CPD (n=19)	**COVID-ARDS (n=13)**	**MIS-C (n=16)**	**Non MIS-C (n=31)**	***P* Value**
Demographics					
Age, years, median (range)	45 (28-69)	62 (19-84)	11 (4-17)	11 (3-18)	
Sex, male (%)	10 (53%)	11 (85%)	7 (44%)	17 (55%)	
Body Mass Index, median (IQR)	na	33.8 (28.4-36.1)	19.1 (17.3-25.5)	19.3 (16.9-22.3)	
Race or Ethnic Group (%)[a]					
Hispanic or Latino	1 (5%)	4 (31%)	4 (25%)	13 (42%)	
Black or African American	0	3 (23%)	7 (44%)	4 (13%)	
White	10 (53%)	2 (15%)	7 (44%)	15 (48%)	
Asian	6 (32%)	0	0	0	
Pacific Islander	2 (11%)	0	0	0	
Other or Unknown	1 (5%)	5 (38%)	1 (6%)	7 (23%)	
Clinical Characteristics					
SARS-CoV-2 PCR Positive (%)[b]	na	13 (100%)	8 (50%)	22 (71%)	
Asymptomatic (%)	na	0	0	15 (48%)	
Days Post Symptom Onset, median (IQR)[c]	24 (19–37)	16 (14–21)	6 (4–7)	29 (17–44)[d]	
SOFA Score[e], median (IQR)[f]	na	11 (9.5–14)	4 (3–7)	na	
Acute Respiratory Distress Syndrome (%)	na	13 (100%)	1 (6%)	1 (3%)	
In-hospital Mortality (%)[g]	na	6 (46%)	0 (0%)	0 (0%)	
Laboratory Results, median (IQR)[f,h,i]					
Absolute Neutrophil Count, x10(3)/μL	na	14.7 (9.1-25.2)	8.9 (7.2-16.4)	5.0 (3.2-8.0)	0.0005
Absolute Lymphocyte Count x10(3)/μL	na	0.9 (0.7-1.4)	0.8 (0.4-1.5)	2.0 (1.3-2.8)	0.0001
Albumin, g/dL	na	3.4 (2.8-3.5)	3.4 (2.6-4.2)	4.6 (4.3-4.9)	$2.6x10^{-7}$
D-dimer, μg/mL	na	7.9(1.7-16.1)	3.1 (1.7-4.3)	na	0.07
Ferritin, ng/mL	na	1933 (971-2693)	521 (298-998)	na	0.002
High Sensitivity CRP, mg/L	na	128 (69-207)	214 (47-300)	na	0.56
Interleukin-6, pg/mL	na	82 (56-315)	219 (54-315)	na	0.63
Lactate Dehydrogenase, U/L	na	777 (638-1379)	268 (229-373)	na	0.0003
Procalcitonin, ng/mL	na	0.4 (0.3-2.0	8.8 (2.1-61.6)	na	0.002
Troponin T, high sensitivity, ng/L	na	24 (16-59)	20 (6-92)	na	0.85

Abbreviations: CPD, convalescent plasma donor; ARDS, Acute Respiratory Distress Syndrome; MIS-C Multisystem Inflammatory Syndrome in Children; SOFA, Sequential Organ Failure Assessment; IQR, Interquartile Range; PCR, Polymerase chain reaction; CRP, C-Reactive Protein

[a] Individuals included in all groups for which they identified

[b] Indeterminate tests were treated as positive

[c] Respiratory symptoms/COVID-19 symptoms for CPD/ARDS groups and symptoms of MIS-C for MIS-C group

[d] Subjective reporting of days post symptom onset for those presenting with symptoms or total days after confirmed COVID-19 exposure (reportable data available for n=16 subjects)

[e] Pediatric and Adult specific scoring applied to groups; not meant for direct comparison

[f] Day of admission for MIS-C, day of intubation for COVID-ARDS, day of PCR or Serology sample testing for Non MIS-C

[g] 30 Day In-hospital mortality, 4 patients remain hospitalized

[h] Values above upper limit entered as; D-Dimer (20 mg/mL), Ferritin (100,000 ng/mL), CRP (200 mg/L), Interleukin-6 (315 pg/mL), Lactate Dehydrogenase (5000 U/L)

[i] Statistical testing for Absolute Neutrophil Count, Absolute Lymphocyte Count and Albumin done via Kruskal-Wallis one-way analysis of variance. Statistical testing for all other laboratory results done by two-tailed Mann-Whitney test. *P* values were calculated to 4 decimal places. Absolute Neutrophil Count and Absolute Lymphocyte Count; n=13 COVID-ARDS, n=16 MIS-C, n=27 Non MIS-C. Albumin; n=13 COVID-ARDS, n=16 MIS-C, n=15 Non MIS-C. D-dimer and Ferritin; n=13 COVID-ARDS, n=16 MIS-C. For High Sensitivity CRP; n=12 COVID-ARDS, n=16 MIS-C. Interleukin-6 and Troponin; n=11 COVID-ARDS, n=16 MIS-C. Lactate Dehydrogenase; n=12 COVID-ARDS, n=15 MIS-C. Procalcitonin; n= 13 COVID-ARDS, n=12 MIS-C.